Investigation of the two-phase convective boiling of HFO-1234yf in a 3.9 mm diameter tube

CrossMark

Ming-Chang Lu, Jing-Rei Tong, Chi-Chuan Wang *

Department of Mechanical Engineering, National Chiao Tung University, Hsinchu 300, Taiwan

ABSTRACT

In this study, the influences of heat flux and mass flux on the two-phase convective boiling heat transfer performance are reported for refrigerants HFO-1234yf and HFC-134a in a 3.9 mm smooth diameter tube. Tests are performed with a saturation temperature of 10 °C. It is found that at lower vapor quality region the nucleate boiling is the dominant heat transfer mechanism while the convective evaporation mechanism takes control at the higher vapor quality region. Both HFC-134a and HFO-1234yf shows similar trend and the difference in heat transfer coefficient between HFO-1234 and HFC-134a is quite small. The comparable heat transfer performance between HFC-134a and HFO-1234yf is attributed to similar physical properties and nucleate boiling contribution. The present test results are in line with some existing reports but are inconsistent with one other study having a tube diameter of 1.1 mm. It is found that the departure of heat transfer coefficients between the available publications is mainly attributed to the different flow phenomena caused by the difference of the channel size and channel geometry. A noticeable deterioration of the heat transfer coefficient for HFO-1234yf is encountered in the microchannel. The pressure drops for HFC-134a is about 5–15% higher than that of HFO-1234yf.

© 2013 Elsevier Ltd. All rights reserved.

1. Introduction

Concerns for chlorofluorocarbons (CFCs) and hydrochlorofluorocarbans (HCFCs) refrigerants casting impact on environment lead to the advent of hydrofluorocarbans (HFCs). Despite HFC refrigerants have no ozone depletion potential (ODP), many of them have a relatively high global warming potential (GWP) which casts significant impact on the environment. For example, HFC-134a is the extensively used refrigerant in air-conditioning and automobile air conditioners (MACs), it has a GWP of 1300 (time horizon of 100 years). As a result, efforts were made to search for new refrigerants that are environmentally benign and can be used to in future air-conditioning and mobile air conditioning systems. Among the candidates, HFO-1234yf is regarded as one of the promising candidates for its GWP is as low as four. The thermophysical properties, cycle performance, and two-phase heat transfer performance of HFO-1234yf are the key parameters to assess the feasibility of using this new refrigerant in air conditioners. The thermophysical properties of refrigerant mixture were similar to those of HFC-134a (Arakawa et al. [1]), thereby offering an opportunity as a drop-in solution for current mobile air conditioners. Normally a drop-in solution yields a lower system performance for lacking optimization in the design process. For instance, Lee and Jung [2] had shown that the coefficient of performance and capacity of HFO-1234yf are up to 2.7% and 4.0% lower than those of HFC-134a, respectively during a typical drop-in experiment. The compressor discharge temperature and the amount of refrigerant charge of HFO-1234yf are 6.5 °C and 10% lower than those of HFC-134a. Analogous results were also reported by Zilio et al. [3] and Navarro-Esbri et al. [4], they also showed a slight decrease in COP for HFO-1234yf system at a same cooling capacity with HFC-134a.

For further optimizing the system performance, further details in designing the heat exchangers (condenser or evaporator) are imperative. As a consequence, information about the two-phase heat transfer convective performance in the evaporator plays a crucial role in optimizing the heat exchangers. However, the published results regarding to the convective evaporation performance of HFO-1234yf is still limited and inconsistent. For instance, Saitoh et al. [5] conducted study for boiling heat transfer of the refrigerant HFO-1234yf flowing in a smooth small-diameter horizontal tube (inner diameter (ID): 2 mm) and Li et al. [6] used similar test facility and identical test tube for comparing the HTC between HFC-32 and HFO-1234yf. Their test results showed that from the low to the high vapor quality region the difference between the heat transfer coefficients of HFO-1234yf and HFC-134a is small, Saitoh et al. [5] attributed this to the small differences in their thermodynamic properties. Recently, Col et al. [7] performed flow boiling of

* Corresponding author.
  E-mail address: ccwang@mail.nctu.edu.tw (C.-C. Wang).

Nomenclature

A_o	outside heat transfer area of the tube, m^2
A_i	nominal inside heat transfer area of the tube, m^2
c_p	specific heat of water, $J\,kg^{-1}\,K^{-1}$
Co	confinement number, $Co = \dfrac{\left(\frac{\sigma}{g(\rho_L - \rho_G)}\right)^{0.5}}{d}$
D	hydraulic diameter at annulus side, m
D_i	inside diameter of the tube, m
D_o	outside diameter of the test tube, m
G	mass flux, $kg\,m^{-2}\,s^{-1}$
g	gravitation constant, N/m
h_i	inside heat transfer coefficient, $W\,m^{-2}\,K^{-1}$
h_o	heat transfer coefficient on the annulus side, $W\,m^{-2}\,K^{-1}$
i_{fg}	latent heat of evaporating vapor, $J\,kg^{-1}$
k	thermal conductivity, $W\,m^{-1}\,K^{-1}$
L	effective heating length, m
LMTD	log mean temperature difference, K
$\dot{m}_{water}$	mass flow rate of the refrigerant, $kg\,s^{-1}$
$\dot{m}_{water}$	mass flow rate of coolant water, $kg\,s^{-1}$
Nu	Nusselt number, dimensionless
p	pressure, kPa
P_r	reduced pressure
Pr	Prandtl mumber, dimensionless
q	heat flux, $W\,m^{-2}$
Q	heat transfer rate, W
Re	Reynolds number, dimensionless
R_w	wall resistance, $K\,W^{-1}$

$T_{water,in}$	inlet temperature of water at annulus side, K
$T_{water,out}$	outlet temperature of water at annulus side, K
T_{sat}	saturation temperature of the refrigerant, K
ΔT	temperature rise on the water coolant, K
ΔT_1	temperature difference, $\Delta T_1 = T_{sat,in} - T_{water,out}$, K
ΔT_2	temperature difference, $\Delta T_2 = T_{sat,out} - T_{water,in}$, K
U_o	overall heat transfer coefficient, $W\,m^{-2}\,K^{-1}$
v	velocity of water at annulus side, $m\,s^{-1}$
x	vapor quality

Greek symbols

ρ_l	density of refrigerant, $kg\,m^{-3}$
μ	dynamic viscosity of refrigerant, $N\,s\,m^{-2}$
σ	surface tension of refrigerant, $N\,m^{-1}$

Subscript

L	liquid phase
G	gas phase
f	water fluid at annulus side
i	inside
in	inlet
o	outside
out	outlet
w	wall
$water$	water

HFO-1234yf in a 1mm diameter circular microchannel and compared to R134a with a saturation temperature of 31 °C. They found that there were no significant differences between the flow boiling performance of R1234yf and R134a. On the other hand, Mortada et al. [8] performed an experiment for HFO-1234yf and HFC-134a in a 1.1 mm rectangular channel with rather small mass flux of 20–100 $kg\,m^{-2}\,s^{-1}$ and heat flux from 2 to 15 $kW\,m^{-2}$. However, their results showed that the HTC for HFO-1234yf is lower than that of HFC-134a as much as 40%. The results are contradictory to the findings of Saitoh et al. [4] and Col et al. [7]. A recent overview about the general two-phase heat transfer characteristics for HFO-1234yf by Wang [9] also reported some inconsistent data in condensation.

In view of the relatively few data associated with the connective boiling performance of HFO-1234yf, it is the objective of this study to report some newly tested data concerning the two-phase convective heat transfer performance. Moreover, there are some contradictory results about the HFO-1234yf and HFC-134a. The present study also aims to elaborate some possible causes about the differences of the existing data.

2. Experimental setup

The schematic of the experimental apparatus is depicted in Fig. 1(a). The test rig is composed of three independent flow loops. Namely, a refrigerant loop, a heating water flow loop and a glycol flow loop. The refrigerant flow loop consists of a variable speed gear pump which delivers subcooled refrigerant to the preheater. The refrigerant pump can provide refrigerant mass fluxes ranging from 100 to 500 $kg\,m^{-2}\,s^{-1}$. A very accurate mass flowmeter is installed between the refrigerant pump and the preheater. Note that the accuracy of the mass flowmeter is generally 0.3% of the test span. The subcooled refrigerant liquid was heated in the preheater to achieve a prescribed evaporator inlet quality before entering the test section. Then, the refrigerant went into the test section to

vaporize. Finally, the two-phase refrigerant was condensed in a shell-and-coil condenser. The horizontal test section is a double-pipe heat exchanger with effective heat transfer length of 0.6 m. Its detailed configuration can be seen from Fig. 1(b). Note that an electrically heated preheater is installed at the upstream of the test section, and the generated two-phase mixtures from the preheater flows into the test section. A 50-mm-thick rubber insulation is wrapped around the double-pipe test section to ensure heat loss to the ambient to be less than 10 W (less than 2% of the heat input) for the test tube. As seen from Fig. 1(b), inside the double-pipe heat exchanger, water flows countercurrently in the test section annulus, while refrigerant is evaporated inside the test tube. The pressure drop of the refrigerant across the test tube was measured by a differential pressure transducer with 10 Pa precision. A magnetic flowmeter was used to record the flowrates of water in the annulus of the test section. The magnetic flowmeter was calibrated in advance with a calibrated accuracy of 0.002 L/s. An absolute pressure transducer was installed at the inlet and exit of the test section with resolution up to 0.1 kPa. During each experiment, the heat flux in the test section is maintained at a desired constant value. Experiments were conducted using a smooth copper tube having an internal diameter of 3.9 mm. Tests were conducted at an evaporation temperature of 10 °C. All of the water and refrigerant temperatures, were measured by RTDs (Pt 100 Ω) having a calibrated accuracy of 0.05 °C. The refrigerant leaving the test section was condensed and subcooled by a glycol circuit. The inlet temperature of the glycol is controlled by a 3 kW low-temperature thermostat. All of the data signals were collected and converted by a data acquisition system (Hybrid recorder). The data acquisition system then transmits the converted signals through USB interface to a host computer for further operation. Uncertainties of the heat transfer coefficients and reported in the present investigation, following the single-sample analysis proposed by Moffat [10], are within ±7.1% of the measured values. The working fluids in this study are HFO-1234yf and HFC-134a.
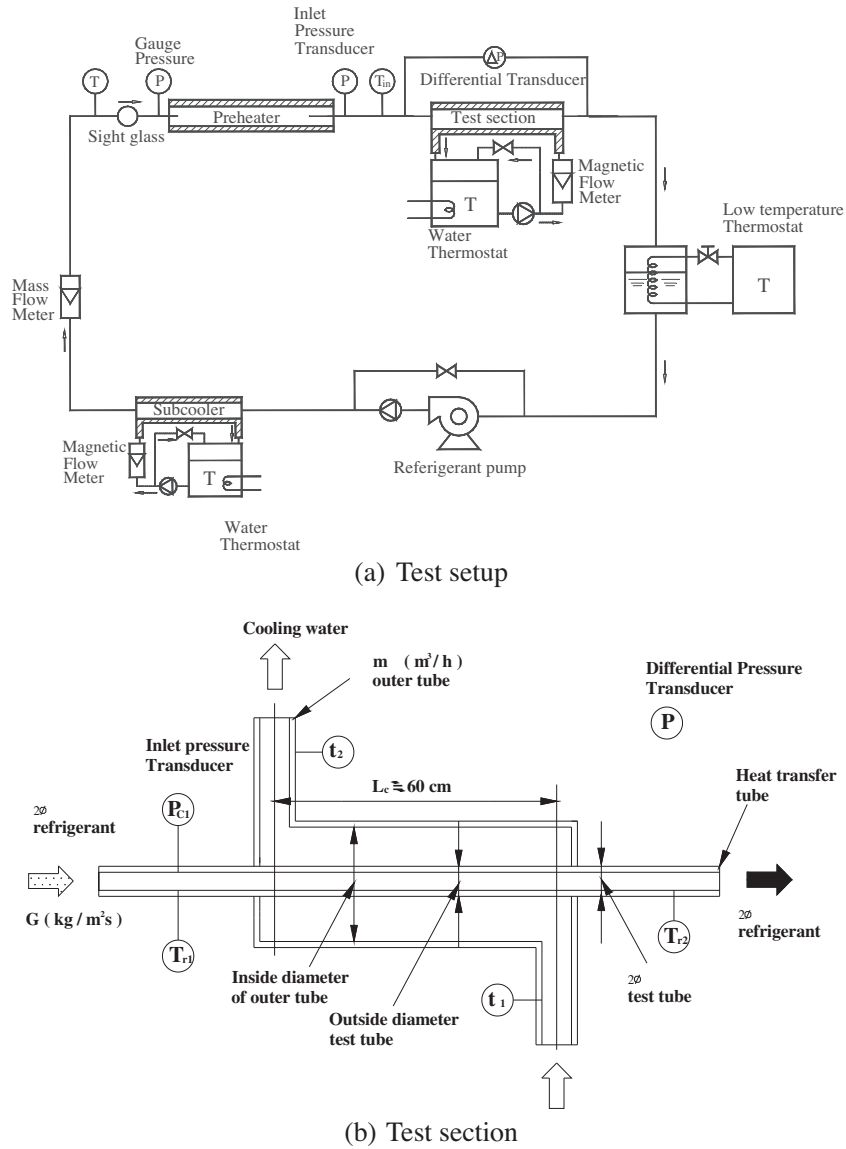
(a) Test setup

(b) Test section

Fig. 1. Schematic of the test facility.

3. Data reduction

The heat duty for the test section was obtained from the flow rate and temperature drop of the water on the annulus according to the relation

$$\dot{Q} = \dot{m}_{water} c_p \Delta T \qquad (1)$$

where c_p is the specific heat of water and ΔT is the temperature difference between water inlet and outlet. $\dot{m}_{water}$ is the mass flowrate of water. The overall heat transfer coefficient was then computed from

$$U_o = \frac{\dot{Q}}{LMTD \times A_o} \qquad (2)$$

where

$$LMTD = \frac{\Delta T_1 - \Delta T_2}{\ln\left(\frac{\Delta T_1}{\Delta T_2}\right)} \qquad (3)$$

$$\Delta T_1 = T_{sat,in} - T_{water,out} \qquad (4)$$

$$\Delta T_2 = T_{sat,out} - T_{water,in} \qquad (5)$$

where $T_{sat,in}$ and $T_{sat,out}$ are the saturation temperatures of the refrigerant in the test section at the inlet and outlet, respectively while $T_{water,in}$ and $T_{water,out}$ denote the inlet and outlet temperature of the water coolant on the annulus. The in-tube heat transfer coefficient was obtained from the thermal resistance equation:

$$\frac{1}{U_o A_o} = \frac{1}{h_o A_o} + R_w + \frac{1}{h_i A_i} \qquad (6)$$

where h_o and h_i represent the average outside and inside heat transfer coefficients, and Rw denotes the wall resistance. In the present calculation, the overall resistance is based on the outer surface area, which is evaluated as $D_o L$, where D_o is the outside diameter of the test tube and L is the effective heat transfer length. The properties on the water side were calculated using average temperature of inlet and outlet bulk fluid temperatures. Note that the heat transfer coefficient and heat flux is based on the inside surface area ($D_i L$). The determination of the inside heat transfer coefficient, h_i, requires knowledge of the outside heat transfer coefficient, h_o. This was accomplished by means of a separate water-to-water tests on the

same apparatus, with subsequent Wilson-plot analyses yielding the individual heat transfer coefficient relationships. The subsequent outline is a typical Wilson plot method applicable to obtain the heat transfer coefficient in the water side.

1. Conduct heat transfer experiments for the test tube (double-tube heat exchanger) with water running in both tube and annulus side. Hence one can calculate the associate heat transfer rate and the logarithmic mean temperature difference, respectively. Notice that it is suggested that the temperature difference in both sides side should be at least 2 °C as suggested for common heat exchanger test to minimize the measurement uncertainty (Wang et al. [11], Wang [12]).

2. The overall resistance can be easily estimated as:

$$R_t = \frac{1}{UA} = \frac{1}{h_i A_i} + R_w + \frac{1}{h_o A_o} \tag{7}$$

3. To obtain the annulus side resistance (heat transfer coefficient) via Wilson plot, it is a must to maintain a fixed thermal resistance in the tube side throughout the test. This can be made possible by fixing an average tube side temperature and a fixed flow rate.

4. The heat transfer performance in annulus side is generally assumed to be the following form:

$$Nu = C_0 Re^a Pr^b \tag{8}$$

Note that an iteration process must be carried out to obtain the correct exponent values of a and b. Initially, one can presume some values of a and b. As a consequence, the heat transfer coefficient in the annulus side is obtained:

$$R_t = \frac{1}{UA} = \frac{1}{h_i A_i} + R_w + \frac{1}{h_o A_o} = \frac{1}{h_o A_o} + C_1$$
$$= \frac{1}{C_0 Re^a Pr^b \frac{k_f}{D} A_o} + C_1 \tag{9}$$

5. Rearranging the overall resistance equation in the following,

$$R_t = \frac{1}{UA} = \frac{1}{C_2 v_f^a} + C_1 \tag{10}$$

The above equation takes the form as

$$y = mx + c \tag{11}$$

With $y = 1/UA$, $m = 1/C_2$, $x = v_f^{-a}$, and $c = C_1$.

6. By changing the velocity in the annulus side, one can have a plot of y vs. x on a linear scale. However, if the plot is not linear, one should adjust the corresponding values of a and b to achieve the linearity. The slope m and the intercept c are then determined from the plot. With m, the heat transfer coefficient in the annulus side can be obtained.

The vapor quality entering the test section (x_{in}) is calculated from the energy balance of the preheater and the quality change in each test section is given by the energy balance

$$\Delta x = \frac{\dot{Q}}{\dot{m}_r i_{fg}} \tag{12}$$

where i_{fg} is the latent heat of refrigerant and $\dot{m}_r$ is the refrigerant mass flowrate. The average quality in each test section is given by:

$$x_{ave} = x_{in} + \frac{\Delta x}{2} \tag{13}$$

4. Results and discussion

Fig. 2 shows the measured heat transfer coefficients between HFC-134a and HFO-1234yf when T_s = 10 °C and G = 200 kg m^{-2} s^{-1} with supplied heat flux being, 5.67, 11.35, and 18.9 kW m^{-2}, respectively. As expected, the heat transfer coefficients (HTC) rise with the vapor quality, indicating appreciably influence of nucleate boiling. On the other hand, the dependence of heat flux for HTCs against vapor quality start to decline when the vapor quality is further increased, suggesting the convective evaporation is in control. The results are applicable for both HFC-134a and HFO-1234yf. In addition, one can see that the measured HTCs for HFC-134a and HFO-1234yf are virtually the same. The results are in line with the measurements of Saitoh et al. [5] and Li et al. [6]. Saitoh et al. [5] conducted convective boiling heat transfer of the refrigerant HFO-1234yf flowing in a smooth small-diameter horizontal tube (inner diameter (ID): 2 mm) and Li et al. [6] used similar test facility and identical test tube for comparing the HTC between HFC-32 and HFO-1234yf. The test tube was heated by direct electrification using a DC power supply connected to two electrodes soldered at the flanges of the two ends of the test tube. Their experimental conditions are T_s = 15 °C, q = 6–24 kW m^{-2}, and G = 100–400 kg m^{-2} s^{-1}. Their measurements also showed that the HTCs are increased with the supplied heat flux at low vapor quality; thus, nucleate boiling is the dominant heat transfer mechanism at the low vapor quality regime. On the other hand, the detectable rise of HTC vs. vapor quality for a low heat flux around 5.7 kW m^{-2} is associated with the change of flow pattern. This is because the annular flow may prevail at high quality region. However, as claimed by the authors [5] who argued that the nucleate boiling is the dominant heat transfer mechanism when q is about 11.5 or 19 kW m^{-2}, thereby showing a moderate change of HTC as the vapor quality is increased. This seems feasible but the relative effect of heat flux, based on the test results of Saitoh et al. [5], is in fact lower. A rough estimation of the HTC with the heat flux dependency is about $h \sim q^{0.42}$ which is generally appreciably lower than the pure nucleate boiling where $h \sim q^{06-0.7}$. In this sense, it is expected that convective evaporation still plays certain minor role rather than pure nucleate boiling. Basically our measurements for
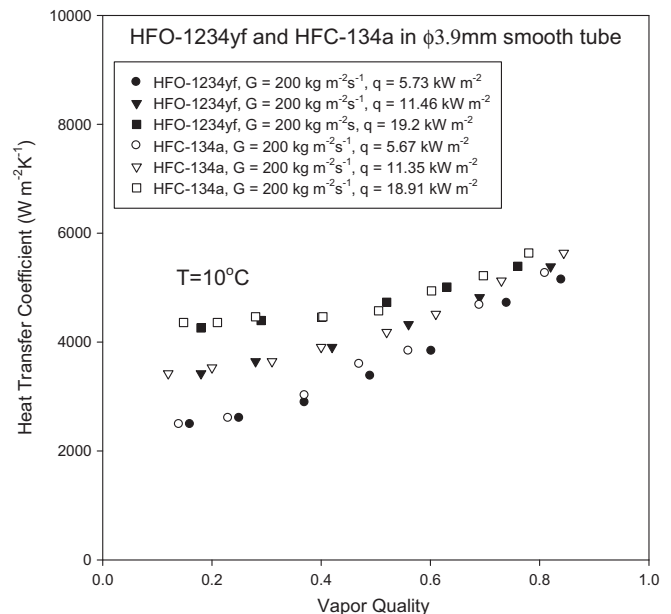

Fig. 2. Test results for heat transfer coefficient for HFC-134a and HFO-1234yf at a saturation temperature of 10 °C and G = 200 kg m^{-2} s^{-1}.

both HFC-134a and HFO-1234yf also reveal a similar heat flux dependence at the lower vapor quality region.

It is interesting to note that the HTCs for HFC-134a and HFO-1234yf are virtually the same regardless the change of heat flux as depicted in Fig. 2. To explain this phenomenon, one must resort to the basic heat transfer mechanisms associated with convective boiling, namely the nucleate boiling and convective evaporation. For nucleate boiling, it is often recognized that three mechanisms, namely bubble agitation (including bubble frequency and site density), vapor–liquid change phenomenon, and evaporation are associated with basic mechanisms of the nucleate boiling heat transfer (Thome, [13]). As shown in Table 1a (Akasaka et al. [1] and Tanaka et al. [14]), the HFO-1234yf has a higher reduced pressure at the same saturation temperature. This is because its critical pressure for HFO-1234yf is about 17% lower than that of HFC-134a. In fact, at a saturation temperature of 40 °C the reduced pressure P_r is approximately 20% higher than that of HFC-134a, thereby leading to a larger activation sites for HFO-1234yf that would boost the heat transfer coefficient.

On the other hand, the smaller bubble departure diameter $\left(\sim \left(\frac{\sigma}{g(\rho_L - \rho_G)} \right)^{0.5}, \sigma : \text{surface tension}, \rho : \text{density} \right)$ of HFO-1234yf implies a lower bubble agitation, and a smaller vapor–liquid change contribution which offset the positive contribution from the higher reduced pressure. A summation of the foregoing effects, consequently, HFC-134a and HFO-1234yf shows nearly identical nucleate boiling HTCs. Therefore, the HTCs for HFC-134a and HFO-1234yf are about the same. To further elaborate about the foregoing qualitative argument, calculation of the HTCs is made using the well-known Chen's correlation [15] applicable to conventional channels for HFC-134a and HFO-1234yf with T_{sat} = 10 °C in a smooth tube having an inner diameter of 10 mm, G = 200 and 400 kg m^{-2} s^{-1} and q = 20 kW m^{-2} as shown in Fig. 3. As clearly shown in the figure, the calculated HTCs for HFC-134a and HFO-1234yf is nearly the same when the vapor quality is less than 0.6, and HFC-134a is marginally higher than those of HFO-1234yf when the vapor quality exceeds 0.6. The results suggest that the difference in HTC between HFC-134a and HFO-1234yf is rather small.

However, as mentioned in the introduction, test results from Mortada et al. [6] for HFO-1234yf and HFC-134a in a 1.1 mm rectangular channel at some rather small mass flux of 20–100 kg m^{-2} s^{-1} and heat flux from 2 to 15 kW m^{-2} showed an opposite trend. Their data indicated the dominance of convective boiling rather than nucleate boiling. There are two possible explanations for this difference. The first is associated with the difference in tube geometry. Notice that present test tube is a round tube while it is rectangular configuration for Mortada et al. [6], and the influence of the liquid film on the heat transfer in a rectangular tube is different from that in a circular tube. Another possible explanation of their results is attributed to the difference in flow phenomenon. As proposed by Kew and Cornwell [16] who took a rigorous approach to define the micro-channels in two-phase flow. They had come out a so-called confinement number (Co), defined as the ratio of the departing bubble diameter to the channel diameter, to determine the transition to micro-channels flow, as below:

$$\text{Co} = \frac{\left(\frac{\sigma}{g(\rho_L - \rho_G)} \right)^{0.5}}{d} \qquad (11)$$
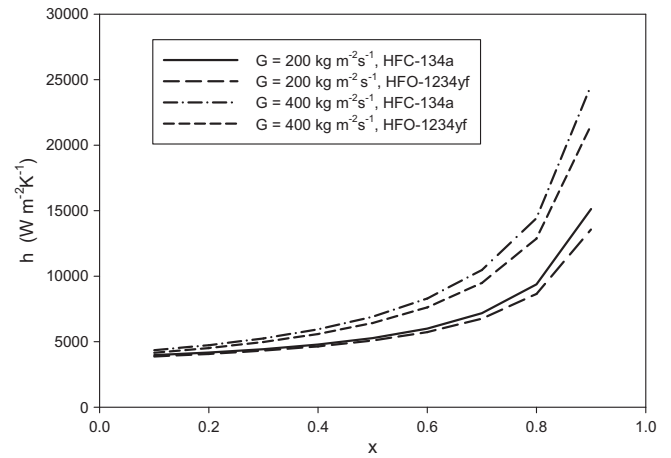

Fig. 3. Comparison of the calculated convective heat transfer coefficient using the Chen's correlation between HFC-134a and HFO-1234yf at a saturation temperature of 10 °C and q = 20 kW m^{-2}.

where σ is the surface tension, ρ_L is the liquid density, ρ_G is the vapor density and d is the inner tube diameter. Based on analysis from some previous data, Kew and Cornwell [16] found that the measured heat transfer coefficients departed appreciably from the conventional channel correlations. They thus chose Co = 0.5 as the transition criteria for microchannel. In this study, the associated Co is around 0.2–0.22 whereas it is about 0.74–0.81 for Mortada et al. [8]. Hence, it explains in part about the different heat transfer behavior between Mortada et al. [8] and the present results. Note that the test results from [8] showed an early dry out at a vapor quality near 0.4 irrespective of the supplied heat flux. The results implied that the annular flow pattern may prevail at an even lower vapor quality, thereby revealing a dominance of the convective boiling. In the meantime, Mortada et al. [8] reported that the measured HTC for HFO-1234yf is lower than that of HFC-134a as much as 40%. The results are contradictory to the findings of Saitoh et al. [5] and the present results where the HTCs for HFC-134a and HFO-1234yf are virtually the same. Again, the difference may be due to the difference in heat transfer characteristics between conventional channels and microchannels. Also, since nucleate boiling is in control in their case, suggesting the aforementioned positive contribution by nucleate boiling for HFO-1234yf has been lifted. In this regard, the flow pattern and physical properties play essential role in the heat transfer performance. The agitation contribution for HFO-1234yf, as depicted in aforementioned discussion, is lowered than that of HFC-134a. In addition, as shown in Table 1b, typically the vapor density of HFC-134a is about 20% lower than that of HFO-1234yf. Hence, the effective vapor velocity for HFC-134a is

Table 1a
Fundamental constants of HFO-1234yf.

	Molecular weight (g mol^{-1})	Critical temperature (K)	Critical pressure (MPa)
HFC-134a	102	374.13	4.07
R-1234yf	114.042	367.85	3.382

Table 1b
Comparison of the physical properties of HFC-134a and HFO-1234yf at T_{sat} = 6 °C and 15 °C.

Property	T_s = 6 °C		T_s = 15 °C	
	R134a	HFO-1234yf	R134a	HFO-1234yf
p (kPa)	363	384.8	493.15	513
ρ_L (kg m^{-3})	1274.6	1156.8	1243	1127.5
ρ_G (kg m^{-3})	17.758	21.52	24.005	28.7
ρ_L (μPa s)	251.28	203.6	224.75	182.5
ρ_G (μPa s)	10.982	11.716	11.365	12.13
k_L (W m^{-1} K^{-1})	0.08936	0.07266	0.08545	0.06925
λ (kJ kg^{-1})	193.98	158.32	186.46	151.95
σ (N m^{-1})	0.010708	0.008564	0.00945	0.0074
$c_{p,L}$ (kJ kg^{-1} K^{-1})	1.358	1.2786	1.3875	1.3125
$c_{p,G}$ (kJ kg^{-1} K^{-1})	0.926	0.9622	0.9735	1.012

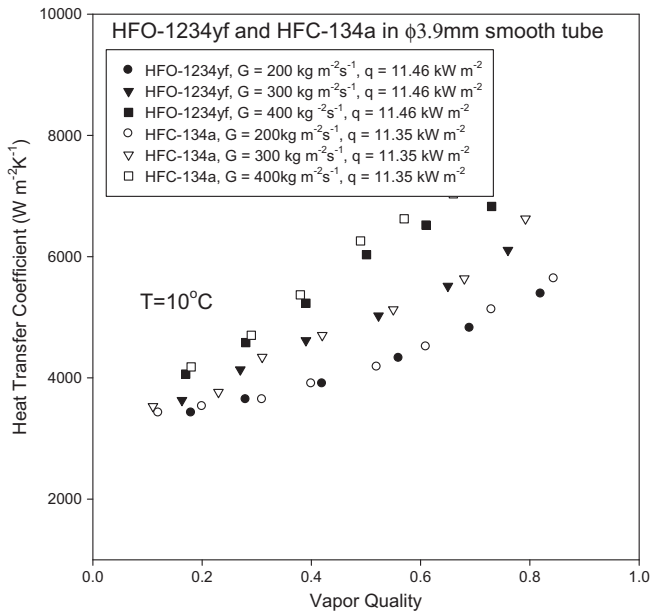**Fig. 4.** Effect of mass flux on HTCs for HFC-134a and HFO-1234yf at a saturation temperature of 10 °C and $q \sim 11.4$ kW m^{-2}.

20% higher than that of HFO-1234yf, implicating a larger convective contribution. In summary of these two effects, it can explain why the heat transfer performance of HFC-134a is superior to that of HFO-1234yf in microchannels. Fig. 4 shows the effect of mass flux on the measured heat transfer coefficients between HFC-134a and HFO-1234yf when $T_s = 10$ °C and $q \sim 11.4$ kW m^{-2} with mass flux being 200, 300, and 400 kW m^{-2}, respectively. At a lower vapor quality of 0.2, the effect of mass flux on HTCs is negligible. The results accord with Fig. 2 where nucleate boiling is the dominant heat transfer mechanism at a lower vapor quality region. Yet the influence of mass flux become more and more pronounced as the vapor quality is increased. Apparently the effect of convective evaporation
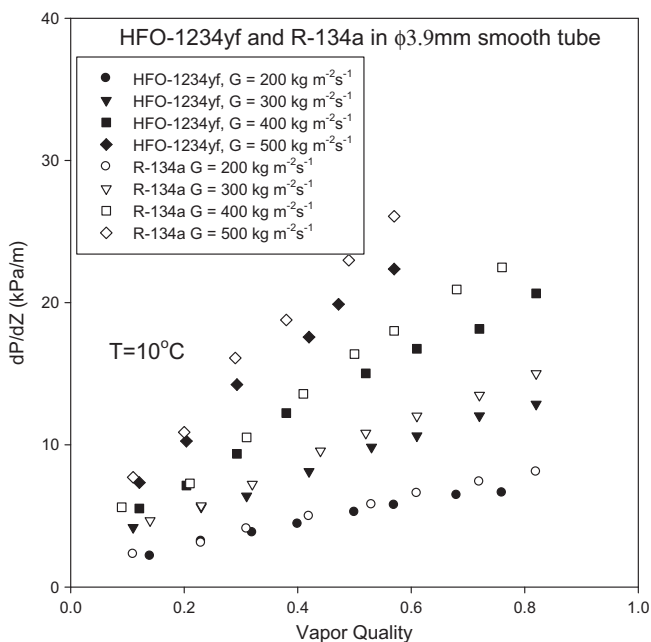

Fig. 5. Effect of mass flux on the pressure drops for HFC-134a and HFO-1234yf at a saturation temperature of 10 °C.

starts to gain control. On the other hand, the HTCs for HFC-134a and HFO-1234yf remain about the same subject to change of mass flux. The test results also indicate an identical heat transfer performance between HFC-134a and HFO-1234yf. The adiabatic two-phase pressure drop of $T_s = 10$ °C for both HFO-1234yf and HFC-134a is depicted in Fig. 5. As expected, the pressure drop is increased with the mass flux and vapor quality. Yet the pressure drops for HFC-134a exceeds those of HFO-1234yf by approximately 5–15%. The higher pressure drops of HFC-134a may be mainly associated with the density difference. It appears that the vapor density for HFC-134a is about 20% lower than that of HFO-1234yf as shown in Table 1b, implying a higher vapor velocity of HFC-134a and a higher pressure drop accordingly.

5. Conclusions

In this study, convective boiling heat transfer performance for refrigerants HFO-1234yf and HFC-134a in a 3.9 mm smooth diameter tube is reported. Tests are performed with a saturation temperature of 10 °C. The influences of heat flux and mass flux on the HTCs are reported in this study. It is found that at lower vapor quality region the nucleate boiling is the controlled mechanism while the convective evaporation mechanism takes control at the higher vapor quality region. Both HFC-134a and HFO-1234yf shows similar trend. Test results also show that the difference in heat transfer coefficient between HFO-1234 and HFC-134a is quite small. The comparable heat transfer performance between HFC-134a and HFO-1234yf is attributed to similar physical properties and the nucleate boiling contribution. This is because the nucleate boiling and convective evaporation contributions of these two refrigerants are about the same provided that the channel size is not too small. Despite the present test results are in line with some existing publications like [4–6], the test results are opposite to those reported by [7]. The departure between the present measurements and [7] is mainly due to the difference in channel geometry and the flow phenomenon. The tube geometry for [4–6] and the present one is of round tube configuration whereas [7] is of rectangular configuration and it is operated in the microchannel regime. The difference in flow phenomenon subject to channel size and channel configuration results in an opposite heat transfer performance. On the other hand, for the present test tube, the effect of mass flux on the HTC becomes more pronounced at higher quality region. This is applicable for both HFC-134a and HFO-1234yf. The pressure drops for HFC-134a is about 5–15% higher than that of HFO-1234yf due to its higher superficial vapor velocity.

Acknowledgements

References

[1] R. Akasaka, K. Tanaka, Y. Higashi, Thermodynamic property modeling for 2,3,3,3-tetrafluoropene (HFO-1234yf), Int. J. Refrig. 33 (2010) 52–60.

[2] Y. Lee, D. Jung, A brief performance comparison of R1234yf and R134a in a bench tester for automobile applications, Appl. Therm. Eng. 35 (2012) 240–242.

[3] C. Zilio, J.S. Brown, G. Schiochet, A. Cavallini, The refrigerant R1234yf in air conditioning systems, Energy 36 (2011) 6110–6120.

[4] J. Navarro-Esbri, J.M. Mendoza-Miranda, A. Mota-Babiloni, A. Barragan-Cervera, J.M. Belman-Flores, Experimental analysis of R1234yf as a drop-in replacement for R134a in a vapor compression system, Int. J. Refrig. 36 (2013) 870–880.

[5] S. Saitoh, C. Dang, Y. Nakamura, E. Hihara, Boiling heat transfer of HFO-1234yf flowing in a smooth small-diameter horizontal tube, Int. J. Refrig. 34 (2011) 1846–1853.

[6] M. Li, C. Dang, E. Hihara, Flow boiling heat transfer of HFO1234yf and R32 refrigerant mixtures in a smooth horizontal tube: Part I. Experimental investigation, Int. J. Heat Mass Transfer 55 (2012) 3437–3446.

[7] D.D. Col, S. Bortolin, D. Torresin, A. Cavallini, Flow boiling of R1234yf in a 1 mm diameter channel, Int. J. Refrig. 36 (2013) 353–362.

[8] S. Mortada, A. Zoughaib, C. Arzano-Daurelle, D. Clodic, Boiling heat transfer and pressure drop of HFC-134a and R-1234yf in minichannels for low mass fluxes, Int. J. Refrig. 35 (2012) 962–973.

[9] C.C. Wang, An overview for the heat transfer performance of HFO-1234yf, Renew. Sustainable Energy Rev. 19 (2013) 444–453.

[10] R.J. Moffat, Describing the uncertainties in experimental results, Exp. Therm. Fluid Sci. 1 (1988) 3–17.

[11] C.C. Wang, R.L. Webb, K.U. Chi, Data reduction of air-side performance of fin-and-tube heat exchangers, Exp. Therm. Fluid Sci. 21 (2000) 228–236.

[12] C.C. Wang, On the heat transfer correlation for membrane distillation, Energy Convers. Manage. 52 (2011) 1968–1973.

[13] J. Thome, Wolverine Engineering Data Book III (Chapter 9).

[14] K. Tanaka, Y. Higashi, Thermodynamic properties of HFO-1234yf(2,3,3,3-tetrafluoropropene), Int. J. Refrig. 33 (2010) 474–479.

[15] J.C. Chen, Correlation for boiling heat transfer to saturated fluids in convective flow, Ind. Eng. Chem. Process Des. Dev. 5 (1966) 322–329.

[16] P.A. Kew, K. Cornwell, Correlations for the prediction of boiling heat transfer in small-diameter channels, Appl. Therm. Eng. 17 (1997) 705–715.